JOURNAL OF BACTERIOLOGY, Aug. 2011, p. 3832–3841 Vol. 193, No. 15
0021-9193/11/$12.00 doi:10.1128/JB.00220-11

Modulation of Rho-Dependent Transcription Termination in *Escherichia coli* by the H-NS Family of Proteins[▽]

Shivalika Saxena and J. Gowrishankar*

Laboratory of Bacterial Genetics, Centre for DNA Fingerprinting and Diagnostics, Hyderabad 500 001, India

Received 16 February 2011/Accepted 7 May 2011

Nascent transcripts in *Escherichia coli* that fail to be simultaneously translated are subject to a factor-dependent mechanism of termination (also termed a polarity) that involves the proteins Rho and NusG. In this study, we found that overexpression of YdgT suppressed the polarity relief phenotypes and restored the efficiency of termination in *rho* or *nusG* mutants. YdgT and Hha belong to the H-NS and StpA family of proteins that repress a large number of genes in Gram-negative bacteria. Variants of H-NS defective in one or the other of its two dimerization domains, but not those defective in DNA binding alone, also conferred a similar suppression phenotype in *rho* and *nusG* mutants. YdgT overexpression was associated with derepression of *proU*, a prototypical H-NS-silenced locus. Polarity relief conferred by *rho* or *nusG* was unaffected in a derivative completely deficient for both H-NS and StpA, although the suppression effects of YdgT or the oligomerization-defective H-NS variants were abolished in this background. Transcription elongation rates *in vivo* were unaffected in any of the suppressor-bearing strains. Finally, the polarity defects of *rho* and *nusG* mutants were exacerbated by Hha and YdgT deficiency. A model is proposed that invokes a novel role for the polymeric architectural scaffold formed on DNA by H-NS and StpA independent of the gene-silencing functions of these nucleoid proteins, in modulating Rho-dependent transcription termination such that interruption of the scaffold (as obtained by expression either of the H-NS oligomerization variants or of YdgT) is associated with improved termination efficiency in the *rho* and *nusG* mutants.

Translation is a cotranscriptional process in both eubacteria and archaebacteria (1, 9, 25, 45, 50), and it has been proposed that such coupling is a defining characteristic of prokaryotic life (34, 64). The maintenance of transcription-translation coupling in a prokaryotic cell would require dynamic inter-regulation between the binding and progression of a pioneer ribosome on the nascent transcript on the one hand and the rate of transcription elongation on the other (9, 45); however, the detailed mechanisms by which such regulation is achieved are not known. Furthermore, in bacteria such as *Escherichia coli*, nascent transcripts that are not simultaneously translated are subject to a mechanism of factor-dependent transcription termination (also referred to as transcriptional polarity) (reviewed in references 1, 6, 15, 40, 44, 47, and 52), so that the occurrence of translation-uncoupled transcription is minimized within the cells (11, 43).

Factor-dependent (also called Rho-dependent) transcription termination is mediated by, among others, the Rho and NusG proteins (1, 6, 15, 39, 40, 44, 47, 52). Although the structures of the two proteins have been determined and several of their biochemical properties have been characterized, the precise mechanisms of their action in transcription termination remain unclear, even controversial. Rho is an RNA-binding protein and possesses RNA-dependent ATPase activity as well as ATP-dependent 5′-3′ translocase/helicase activity on RNA. Recently, Rho has also been reported to bind RNA polymerase (21). NusG has two domains that bind Rho and RNA polymerase, respectively (13, 36). The Rho-binding domain in NusG has also recently been shown to interact with the S10 protein subunit of the ribosome, which has implications for the mechanism by which translation-uncoupled nascent transcripts may be subject to termination of their synthesis (9). Although null mutations in *rho* or *nusG* confer inviability in wild-type *E. coli* (11), missense mutations in the two genes are known that confer a transcription termination-defective (that is, polarity relief) phenotype (1, 12, 13, 27, 36).

In the present study, we found that overexpression of the protein YdgT restores transcriptional polarity in the *rho* and *nusG* mutants and, furthermore, that the combination of *rho*, *ydgT*, and *hha* mutations confers extreme sickness in *E. coli*. YdgT (also called Cnu [30]) and Hha belong to the H-NS family of proteins (33), whose prototypic member H-NS participates in both regulation of transcription initiation and nucleoid structure (reviewed in references 16, 20, 23, and 59). Genetic, biophysical, and structural studies have shown that the 137-amino acid H-NS protein possesses two separate dimerization interfaces, between approximately residues 2 and 47 and residues 58 and 84, respectively, and a third C-terminal DNA-binding domain between residues 92 and 137 (3, 5, 8, 22, 54, 57, 58). (Amino acid residues in H-NS are numbered here beginning from the N-terminal methionine as 1 [65], even though this residue is posttranslationally removed from the mature protein.) The presence of the two dimerization interfaces allows H-NS to assemble (either alone or with its paralogous partner StpA [53, 55, 60, 65, 67]) into a helical polymeric scaffold around which DNA is bound (3, 22). Binding of H-NS to DNA results in several structural (including supercoiling) alterations that have been variously referred to as bending, bridging, coating, looping, and stiffening of the DNA (16, 20,

* Corresponding author. Mailing address: Centre for DNA Fingerprinting and Diagnostics, Building 7, Gruhakalpa, 5-4-399/B, Nampally, Hyderabad 500 001, India. Phone: 91-40-2474 9445. Fax: 91-40-2474 9448. E-mail: shankar@cdfd.org.in.

▽ Published ahead of print on 20 May 2011.

23, 32, 39, 61). YdgT and Hha bear structural resemblance to, and also interact with, the N-terminal oligomerization domains of H-NS and StpA; in this manner, YdgT and Hha are believed to modulate the DNA-binding and nucleoid-organizing properties of H-NS and StpA even though they do not bind DNA by themselves (23, 30, 33, 38, 42, 55).

Certain mutations in *hns* had previously also been reported to modulate Rho-dependent transcription termination (27). In the present study, we found that the expression of H-NS variants defective in one or the other of the oligomerization interfaces, but not in the DNA-binding domain alone, was associated with restoration of transcriptional polarity in *rho* and *nusG* mutants. A model is proposed in which it is the architecture of the polymeric scaffold assembly of H-NS and StpA that determines the efficiency of transcription termination in *rho* and *nusG* mutant strains.

MATERIALS AND METHODS

Growth media, bacterial strains, and plasmids. The routine defined and rich growth media were, respectively, minimal A medium (supplemented with glucose at 0.2% or other indicated C source and amino acids, as required, at 40 μg/ml) and Luria-Bertani (LB) medium (35). Strains for *proU-lac* expression measurements were grown in LBON medium (that is, LB with NaCl omitted) (18). Unless otherwise indicated, the growth temperature was 37°C. Kanamycin (Kan), ampicillin (Amp), and trimethoprim (Tp) were each used at 50 μg/ml, and tetracycline (Tet) and chloramphenicol (Cm) were each used at 15 μg/ml. IPTG (isopropyl-β-D-thiogalactopyranoside) was used at 0.5 mM.

The *E. coli* K-12 strains used in the study are described in Table 1. Plasmids described previously included the following (with salient features in parentheses): the vectors pWSK30 (pSC101 replicon, Amp resistant [Amp^r]) (62), pBAD18 (ColE1 replicon, Amp^r, for L-arabinose [Ara]-induced expression of target genes) (26), pACYC184 (p15A replicon, Tet^r Cm^r) (14), and pTrc99A (ColE1 replicon, Amp^r, for IPTG-induced expression of target genes (2); pCP20 (pSC101-based Ts replicon, Cm^r Amp^r, for *in vivo* expression of Flp recombinase) (17); pHYD272 (single-copy-number IncW replicon carrying *proU-lac* transcriptional fusion, Tp^r) (18); and a set of plasmids described by Williams et al. (65) comprising the vector pLG339 (pSC101 replicon, Kan^r) and its derivatives carrying *hns*$^+$ or one of the following *hns* alleles encoding the dominant-negative H-NS substitution variants L26P, E53G/T55P, Y97C, P116S, or I119T or the truncation variant referred to as Δ64 (an allele which has a frameshifting 1-bp deletion mutation after codon 63 in the gene) and designated accordingly with a pLG- prefix.

Plasmid pHYD1622 (Cm^r Amp^s) is derived from the plasmid pHYD1201 (Amp^r Cm^s) previously described (27) and carries the *rho*$^+$ gene on a replicon that is IPTG dependent for replication (K. Anupama, unpublished data). Plasmid pHYD2509 was obtained by subcloning an EcoRI fragment encoding H-NSΔ64 (genomic coordinates from bp 1291698 to 1292238 [48]) from the corresponding pLG plasmid of Williams et al. (65) into the EcoRI site of pWSK30. The gene encoding YdgT (with its native ribosome-binding site) was PCR amplified from the chromosomal *ydgT* locus with the pair of primers 5′-CCCTTTGGTAT*GAATTC*TTTTATGGACCT-3′ and 5′-ATAACCGATCG *AAGCTT*TCTTTATTGGACA-3′ (the EcoRI and HindIII sites, respectively, are italicized in the two primer sequences) and cloned as a 239-bp fragment (genomic nucleotide coordinates 1702957 to 1703190 [48]) into the EcoRI-HindIII sites of pBAD18 and pTrc99A to generate plasmids pHYD2525 and pHYD2528, respectively. In an identical fashion, a derivative of pTrc99A was constructed that carries a 223-bp gene fragment designed to encode H-NSΔ64 (genomic nucleotide coordinates 1291956 to 1292172 [48]), following PCR amplification from the chromosomal *hns* locus with the primers 5′-TATTACCTC AA*GAATTC*ACCCCAATATAAG-3′ and 5′-TACCGTCAGCGA*AAGCTT*AT TCGCGATATTG-3′, to generate plasmid pHYD2526. The presence of the underlined TTA sequence in the last primer resulted in insertion of a TAA nonsense mutation immediately after codon 63 of the truncated *hns* gene in the cloned PCR amplicon. For convenience, the variant encoded by this construct is also referred to as H-NSΔ64, since its properties were identical to that encoded by the 1-bp deletion allele of Williams et al. (65) described above. All plasmid inserts obtained after PCR amplification were validated by DNA sequencing.

TABLE 1. *E. coli* K-12 strains

Strain[a]	Genotype[b]
MG1655	Wild type
RS353	Δ(*argF-lac*)*U169 rpsL150 relA1 flbB5301 deoC1 ptsF25*
RS445	RS353 *araD139 galEp3*, λRS88 lysogen carrying P_{lac}-*lacZYA*
GJ3171	MG1655 *rho*(*A243E*)
GJ5146	GJ5147 *rho*(*A243E*)
GJ5147	RS353 *araD139 galEp3*, λRS45 lysogen carrying P_{lac}-H-19Bt_{R1}-*lacZYA*
GJ5153	GJ5147 *nusG*(*G146D*)
GJ6504	MG1655 *lacI lacZ*$_{U118}$(Am) *trpR55 trpE9777*(Fr)
GJ6509	GJ6504 *rho*(*A243E*)
GJ6511	GJ6504 *nusG*(*G146D*)
GJ7438	GJ6511 Δ*stpA*
GJ10570	RS445 *rho*(*A243E*)
GJ10571	RS445 *nusG*(*G146D*)
GJ10606	GJ6509 *hns-1001*::Kan
GJ10607	GJ6511 *hns-1001*::Kan
GJ10646	GJ6511 Δ*hha*
GJ10649	GJ6511 Δ*ydgT*
GJ10663	GJ6509 Δ*stpA hns-1001*::Kan
GJ10664	GJ6511 Δ*stpA hns-1001*::Kan
GJ10676	GJ6511 Δ*ydgT* Δ*hha*::Kan
GJ10729	MG1655 *nusG*(*G146D*)
GJ10738	GJ6509 Δ*pcnB*::Kan
GJ10740	GJ6509 *hns-205*::Tn*10*
GJ10741	GJ6511 *hns-205*::Tn*10*
GJ10742	RS353 *hns-205*::Tn*10*
GJ10743	RS353 *hns-1001*::Kan
GJ10752	GJ6509 Δ*ydgT* Δ*hha*::Kan
GJ10764	GJ5147 Δ*hha*::Kan
GJ10765	RS445 Δ*hha*::Kan
GJ10766	GJ5153 Δ*hha*::Kan
GJ10767	GJ10571 Δ*hha*::Kan
GJ10781	GJ10570 Δ*hha*::Kan
GJ10782	GJ5153 Δ*hha*::Kan
GJ10783	GJ10570 Δ*ydgT*::Kan
GJ10784	GJ10571 Δ*ydgT*::Kan
GJ10785	GJ5146 Δ*hha*::Kan
GJ10786	GJ5147 Δ*ydgT*::Kan
GJ10787	RS445 Δ*ydgT*::Kan
GJ10788	GJ5146 Δ*ydgT*::Kan
GJ10789	GJ5147 Δ*hha* Δ*ydgT*::Kan
GJ10790	RS445 Δ*hha* Δ*ydgT*::Kan
GJ10791	GJ10571 Δ*hha* Δ*ydgT*::Kan
GJ10792	GJ5153 Δ*hha* Δ*ydgT*::Kan

[a] Strain MG1655 was from our laboratory stock collection. Strains described earlier include GJ3171 (27) and RS353 and RS445 (12). Strain GJ5147 is an Ilv$^+$ derivative of GJ3073 (12). Strains GJ6504, GJ6509, and GJ6511 were constructed by S. Aisha (unpublished data). All other strains were constructed in this study.

[b] Genotype designations are as described previously (7). All strains are F$^-$. References or sources for the mutations that were introduced by transduction into the strains are as follows: *rho*(*A243E*) (interchangeably also designated as *rho-4*) and *nusG*(*G146D*) (27); *hns-1001*::Kan (Tn*5*seq1 insertion in codon 20 of *hns*) (28); and *hns-205*::Tn*10* (Tn*10* insertion in codon 92 of *hns*) (19). The Δ*pcnB*, Δ*stpA*, Δ*hha*, and Δ*ydgT* mutations were introduced as Kan^r deletion-insertion mutations from the Keio knockout collection (4) and, where necessary, the Kan^r marker was then excised by site-specific recombination with the aid of plasmid pCP20, as described previously (17). The latter mutations are shown without the Kan^r designation in the table.

The plasmids bearing *ydgT* that were identified from the *E. coli* genomic library in pACYC184 are described in Fig. 1.

Screening for *rho* and *nusG* phenotypes. Relief of transcriptional polarity associated with the *rho-4* [interchangeably referred to also as *rho*(*A243E*) (27)] and the *nusG*(*G146D*) mutations was scored in three ways: the ability of a *trpE9777* (Frameshift) mutant to utilize anthranilate (Anth) at 20 μg/ml as a substitute for tryptophan (Trp) for meeting its auxotrophic requirement; the

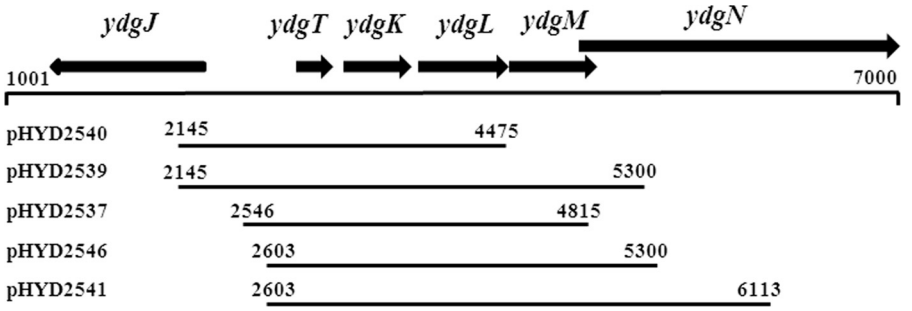

FIG. 1. Extent of chromosomal regions carried by various *ydgT*-bearing plasmid clones in survivor transformants of *rho* and *nusG* mutants. The plasmids are from a library comprised of partial Sau3A1-digested genomic fragments cloned into the BamHI site of pACYC184. The physical map of genes in the vicinity of *ydgT* is depicted at the top (48), and each of the lines aligned beneath the map represents the extent of chromosomal DNA cloned into a plasmid whose numerical designation is indicated alongside. Nucleotide coordinates (48) marked both on the map and for the ends of the inserts refer to the 1,700-kb region of the *E. coli* genome (that is, 2603 represents genomic coordinate 1702603, and so on).

ability of a $lacZ_{U118}$ (Amber) mutant to grow on 0.2% melibiose as sole carbon source at 39°C; and an increase in the ratio of expression of β-galactosidase from a derepressed P_{lac}-t_{R1}-*lacZ* fusion construct integrated in single copy into the chromosome (where t_{R1} is one of the Rho-dependent terminators from lambdoid phage H19B) to that from an equivalent P_{lac}-*lacZ* fusion construct (without t_{R1}) (12, 13). In the first two assays, cultures were either spotted at serial dilutions, or plated to observe growth of single colonies, on the indicated media.

Another phenotype of *rho* and *nusG* mutants used in the present study was that of lethality after 24 to 40 h of transformation with plasmid pACYC184, which has been attributed to increased occurrence of chromosomal R-loops and consequential over-replication of the plasmid in the mutants (25, 27).

Immunoblot analysis of *in vivo* Rho and NusG levels. Cells from cultures grown to mid-log phase were washed once in phosphate-buffered saline, and cell extracts were prepared by sonication. Procedures for protein estimation, electrophoresis through sodium dodecyl sulfate-polyacrylamide gels (10% for Rho, 15% for NusG), electroblotting to a polyvinylidene difluoride membrane, Ponceau-S staining, and reactions with primary and secondary antibodies were essentially as described previously (49). Primary anti-Rho and anti-NusG antibodies (mouse, polyclonal) for the detection of Rho and NusG levels, respectively, were kindly provided by Ranjan Sen. Binding of secondary anti-mouse IgG antibody (goat, peroxidase-conjugated) was visualized with the aid of a chemiluminescence detection system according to the manufacturer's protocol (Sigma Chemical Co., St. Louis, MO). Ponceau-S staining of the membrane after electroblotting was used to control for differences if any across lanes in protein loading and blotting efficiency.

Other methods. Procedures for P1 transduction (35), *in vitro* DNA manipulations and transformation (49), and β-galactosidase assays (35) were as described previously. *In vivo* transcription elongation rate measurements at *lacZ* were performed as described by Jin et al. (29). Junction sequences in clones of the genomic library in pACYC184 were determined with the aid of a pair of vector-based *tet* primers: 5′-CGCCGAAACAAGCGCTCATGAGCC-3′ and 5′-CTATGCGCACCCGTTCTCGGAGCAC-3′.

RESULTS

Identification of *ydgT* as multicopy suppressor of *rho* and *nusG*. It has been reported earlier that transcription termination-defective *rho* and *nusG* mutants are killed upon transformation with certain plasmids of the ColE1 family, such as pACYC184 or pUC19, because of plasmid over-replication (27). In order to obtain multicopy suppressors of *rho* and *nusG*, an *E. coli* genomic library in plasmid pACYC184 was introduced into the strains GJ6509 (*rho*) and GJ6511 (*nusG*). The vast majority of the transformant colonies were inviable after 40 h of incubation, and the few survivor transformants were then tested for transcriptional polarity relief at *lacZ* and *trpE* loci carrying, respectively, premature nonsense and frameshift mutations. At least five independent plasmid clones were identified that were both nonlethal (despite being pACYC184 derivatives) and able to confer suppression of transcriptional polarity relief at *lacZ* and *trpE* in the *rho* and *nusG* backgrounds; junction-sequencing data revealed that all of them carried varying extents of the *ydgTKLMN* operon (Fig. 1). One representative plasmid from this experiment pHYD2546 (with a 2.7-kb insert) was shown also to suppress transcriptional polarity relief at the t_{R1} terminator of lambdoid phage H19B in both *rho* and *nusG* mutants from ca. 35% to ca. 15%, similar to that obtained upon expression of the H-NS variant Δ64 (Table 2).

As stated above, it is known that certain *hns* mutations are

TABLE 2. Suppression by H-NSΔ64 or YdgT expression of polarity relief at phage t_{R1} terminator in *rho* and *nusG* mutants

Plasmid (feature)	Mean ± SE[a]								
	Wild type			*rho*			*nusG*		
	$-t_{R1}$ (A)	$+t_{R1}$ (B)	% B/A	$-t_{R1}$ (A)	$+t_{R1}$ (B)	% B/A	$-t_{R1}$ (A)	$+t_{R1}$ (B)	% B/A
Nil	9,516 ± 2,178	381 ± 71	4 ± 1	7,233 ± 3,028	2,284 ± 695	32 ± 5	5,686 ± 1,781	1,723 ± 635	30 ± 8
pLG339 (vector)	10,616 ± 845	536 ± 238	5 ± 2	6,967 ± 2,153	2,889 ± 818	41 ± 1	7,463 ± 820	2,769 ± 1,008	37 ± 10
pLG-Δ64 (H-NSΔ64)	8,101 ± 3,159	564 ± 63	7 ± 2	9,059 ± 3,442	1,626 ± 351	18 ± 3	7,761 ± 2,523	1,309 ± 334	17 ± 2
pHYD2546 (YdgT)	4,171 ± 36	211 ± 8	5 ± 0	4,359 ± 511	356 ± 59	8 ± 2	3,059 ± 101	449 ± 85	15 ± 3

[a] The specific activities of β-galactosidase were determined after growth in LB medium of wild-type, *rho*, and *nusG* strains without ($-t_{R1}$ [A]) or with ($+t_{R1}$ [B]) the phage t_{R1} terminator upstream of the *lacZ* reporter gene and carrying the plasmids as indicated. The strains were, respectively, as follows: RS445, GJ10570, and GJ10571 ($-t_{R1}$) and GJ5147, GJ5146, and GJ5153 ($+t_{R1}$). The B/A ratios given in the table are a measure of transcriptional readthrough or polarity relief at the t_{R1} terminator.

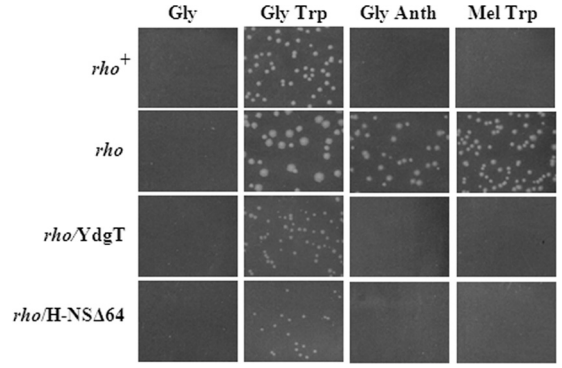

FIG. 2. Relief of transcriptional polarity in *rho* mutant and its suppression by H-NSΔ64 and YdgT. Strains GJ6504 (*rho*$^+$), GJ10738 (*rho*), GJ10738/pHYD2528 (*rho*/pTrc:YdgT), and GJ10738/pHYD2526 (*rho*/pTrc:H-NSΔ64) were plated at a suitable dilution on a set of four minimal A-based plates, as shown. Gly, 0.4% glycerol (C source); Mel, melibiose (C source). The Mel Trp plates were incubated at 39°C.

suppressors of *rho* and *nusG* (27) and, since YdgT is an interacting partner of H-NS (30, 33, 42), we tested whether it is the presence of YdgT in the plasmid derivatives that was responsible for the suppression phenotype. The minimal *ydgT* construct, as well as the gene fragment encoding H-NSΔ64 as a positive control, was cloned downstream of the IPTG-inducible *trc* promoter in the ColE1-plasmid vector pTrc99A. The vector by itself conferred lethality in *rho* or *nusG* strains but not in their *pcnB* derivatives (consistent with the earlier finding that plasmid copy number reduction mediated by *pcnB* mutation suppresses ColE1 plasmid lethality in *rho* and *nusG* mutants [27]). On the other hand, the plasmids expressing H-NSΔ64 (pHYD2526) or YdgT (pHYD2528) were viable in both *pcnB*$^+$ and Δ*pcnB* derivatives of the *rho* and *nusG* strains (data not shown), and their presence was also associated with suppression of transcriptional polarity relief (see Fig. 2 for data on *rho* suppression). Similar results were obtained with plasmid pHYD2525 carrying the minimal *ydgT* construct downstream of $P_{ara,}$ with the difference that the phenotypes elicited here were inducer (0.2% Ara) dependent (data not shown). These data indicate that YdgT overexpression is correlated with restoration of the efficiency of Rho-dependent termination in *rho* and *nusG* mutants.

The data in Table 2 for *lac* fusion strains with or without the phage t_{R1} terminator also showed that, unlike the situation with H-NSΔ64, YdgT overexpression is associated with a general 2-fold reduction in β-galactosidase levels even in derivatives without the t_{R1} terminator. However, the explanation for this is at present not known.

We also attempted to test whether overexpression of Hha, the functionally related YdgT paralog (33), affects Rho-dependent termination. These experiments were undertaken with both pTrc99A- and pBAD18-derived plasmids carrying *hha* downstream of the P_{trc} and P_{ara} promoters, respectively, but they were inconclusive because Hha overexpression was toxic even in the wild-type strain (data not shown), as reported earlier (24). This toxicity was not alleviated by coexpression of the gene *tomB* upstream of *hha* in the same operon (data not shown), which has been claimed to be an antidote to Hha's toxicity (24).

H-NS perturbations affecting Rho-dependent termination. It had been demonstrated earlier that certain mutations in *hns*, but not Δ*hns* itself, suppress *rho*- and *nusG*-associated phenotypes (27), and this phenomenon was examined in detail in the present study. Genetic suppression was tested as a reversal of the phenotype of transcriptional polarity relief at the *trpE9777* locus, as well as that of lethality with plasmid pACYC184, as described above.

Williams et al. (65) have described a set of dominant-negative variants of H-NS and, when several of these were tested, Δ64 was able to suppress the Anth$^+$ phenotype conferred by the *rho* mutation in the *trpE* (Frameshift) derivative nearly completely and two others (L26P and E53G/T55P) to a smaller extent, whereas three more (Y97C, P116S, and I119T) were largely ineffective for suppression (Fig. 3). An H-NS variant truncated after amino acid residue 91 (Δ92) is also known to be dominant negative (57, 58), and we found that the chromosomal *hns-205*::Tn*10* allele which encodes a Δ93 variant (19) was ineffective for *rho* suppression at *trpE9777*, as also was the null allele of *hns* itself (*hns-1001*) (Fig. 3). This dichotomy in the ability of the different *hns* mutations to suppress transcriptional polarity relief in the *rho* and *nusG* mutant was recapitulated also for suppression of lethality with plasmid pACYC184 in both *rho* and *nusG* derivatives (viable with Δ64, L26P, and E53G/T55P; inviable with Δ93, Y97C, P116S, I119T, and *hns-1001*) (Table 3).

Derepression of *proU-lac* with H-NS and YdgT perturbations. H-NS is best known for its ability to repress or silence the expression of a large number of genes in *E. coli* and other enterobacteria by acting at the level of transcription initiation of these genes. This function of H-NS is dependent on its ability to bind DNA and to oligomerize, leading to the bridging together of otherwise distant DNA segments on the chromosome (reviewed in references 20, 23, 39, and 55). The osmotically regulated *proU* operon in *E. coli* is a prototypical example of an H-NS-regulated locus (46, 57, 58, 65), and we measured expression of a *proU-lac* transcriptional fusion in the various (*rho*$^+$ *nusG*$^+$) derivatives perturbed for H-NS or YdgT.

In conformity with data from earlier studies (18, 46, 57, 58, 65), *proU* transcription was very low upon growth of the *hns*$^+$ strain in a low-osmolarity medium, whereas it was derepressed approximately 5- to 10-fold in the merodiploid (with chromosomal *hns*$^+$) strains carrying any of the plasmid-borne dominant-negative *hns* mutations of Williams et al. (65) and 35- to 70-fold in the haploid *hns* mutants *hns-1001* (null) or *hns-205*::Tn*10* (encoding H-NSΔ93) (Table 3). Therefore, these results confirmed that, although the H-NS variants fall into two categories with respect to their ability to suppress *rho* and *nusG*, all of them are defective for silencing of *proU* expression to equivalent extents.

As with the *hns* mutations, we found YdgT overexpression also to be associated with pronounced derepression of *proU-lac* expression at low osmolarity. Thus, in derivatives of a *proU-lac* strain (RS353/pHYD272) bearing plasmids pHYD2525 (P_{ara}-*ydgT*) or pHYD2528 (P_{trc}-*ydgT*) grown in LBON medium with inducer supplementation (L-arabinose at 0.2% or IPTG, as appropriate), the β-galactosidase specific activities were 17 ± 4 U and 64 ± 11 U, respectively, compared to control values of approximately 5 ± 0 U and 8 ± 1 U in the corresponding

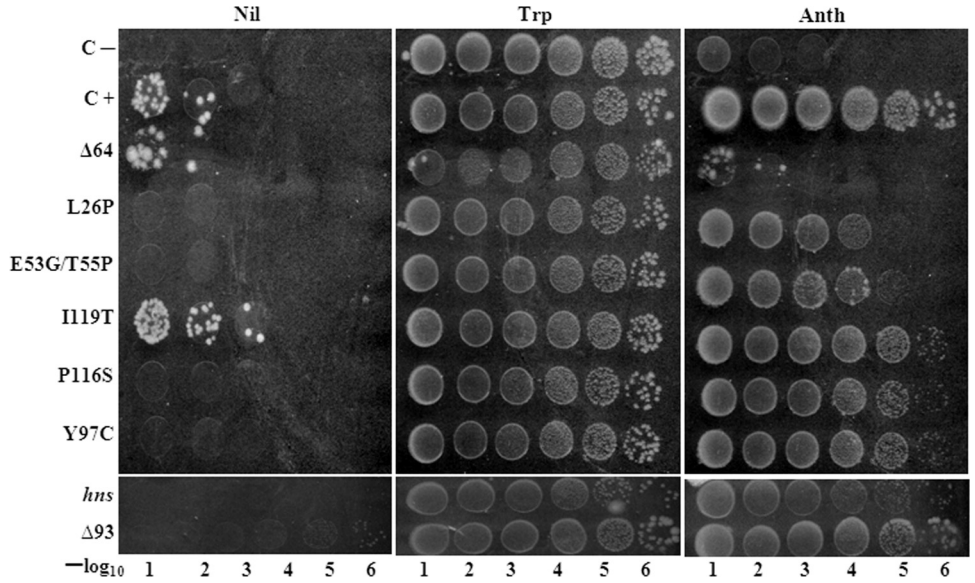

FIG. 3. Effect of different H-NS variants (expressed from the corresponding pLG- plasmids) on polarity relief at *trpE9777* (Frameshift) locus of *rho* mutant GJ6509. Derivatives were spotted at the indicated dilutions on Kan-containing glucose-minimal A plates with nil, Trp, or Anth supplementation as marked. Negative (C−) and positive (C+) controls are the vector (pLG339)-bearing derivatives of GJ6504 (*rho*$^+$) and GJ6509 (*rho*), respectively. The bottom two rows (marked *hns* and Δ93) are of strains GJ10606 (*rho hns-1001*) and GJ10740 (*rho hns-205*::Tn*10*), on plates without Kan supplementation.

vector-bearing derivatives pBAD18 and pTrc99A. These data establish that YdgT overexpression perturbs H-NS-mediated silencing of gene expression in *E. coli*.

Chromosomal requirements for *rho* and *nusG* suppression by H-NS variants or YdgT overexpression. We then determined whether the suppressor effects of the H-NS variants and of YdgT were dependent on the functional state of the chromosomal *hns*, *stpA*, *hha*, and *ydgT* loci. The *rho* and *nusG* derivatives of an *hns-1001* Δ*stpA* strain continued to exhibit transcriptional polarity relief (see Fig. 4 for *nusG*) but, inter-

TABLE 3. Effects of different H-NS variants on *proU-lac* expression (in wild-type strain) and pACYC184 lethality in *rho* and *nusG* mutants

H-NS variant[a]	Mean *proU-lac* expression ± SE[b]	pACYC184 phenotype[c] in:	
		rho strain	*nusG* strain
+	3 ± 1	I	I
Null	215 ± 4	I	I
Δ93	113 ± 27	I	I
+/Δ64	14 ± 0	V	V
+/L26P	23 ± 2	V	V
+/E53G-T55P	19 ± 1	V	V
+/Y97C	21 ± 0	I	I
+/P116S	26 ± 3	I	I
+/I119T	28 ± 0	I	I

[a] Strains for different H-NS variants employed were (in order, wild-type, *rho*, and *nusG* backgrounds): + (RS353, GJ6509, and GJ6511); null, that is, *hns-1001* (GJ10743, GJ10606, and GJ10607); and Δ93, that is, *hns205*::Tn*10* (GJ10742, GJ10740, and GJ10741). In merodiploid derivatives, the dominant-negative H-NS variants were expressed from the corresponding pLG- plasmids.

[b] Values are presented as the specific activities of β-galactosidase in derivatives of the indicated wild-type strains carrying the *proU-lac* plasmid pHYD272 after growth in LBON medium.

[c] Phenotypes of viability (V) or inviability (I) were scored at 40 h after transformation of the *rho* and *nusG* derivatives with pACYC184.

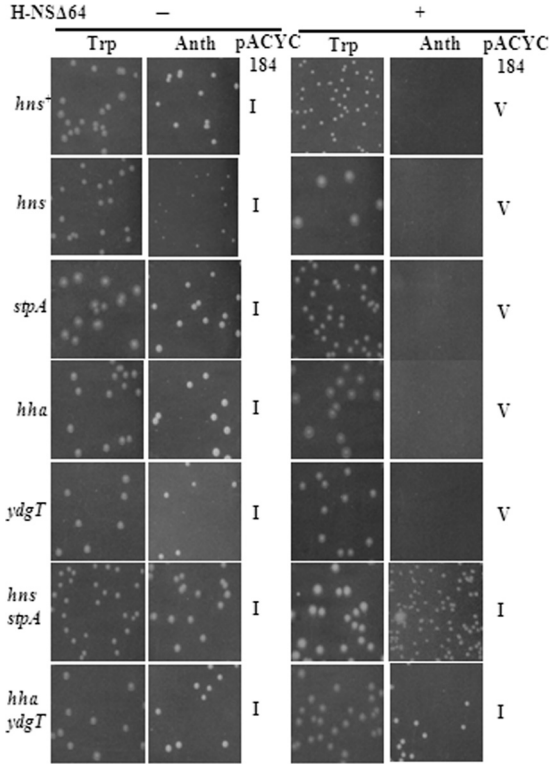

FIG. 4. Chromosomal mutations that affect suppression by H-NSΔ64 of transcriptional polarity relief in *nusG* mutant. The *nusG* strains GJ6511 (*hns*$^+$), GJ10607 (*hns-1001*, marked *hns* in the figure), GJ7438 (*stpA*), GJ10646 (*hha*), GJ10649 (*ydgT*), GJ10664 (*hns stpA*), and GJ10676 (*hha ydgT*), as well as their derivatives carrying pHYD2509 that expresses H-NSΔ64, were plated at a suitable dilution on a pair of glucose-minimal A plates supplemented with 19 amino acids (excluding Trp) and Trp or Anth, as indicated. Also marked are the phenotypes of viability (V) or inviability (I) of the derivatives at 40 h after transformation with pACYC184.

TABLE 4. Effects of Δ*hha* and Δ*ydgT* mutations on polarity relief at phage t_{R1} terminator in *rho* and *nusG* mutants

hha and *ydgT* genotype		Mean ± SE[a]								
		Wild type strain			*rho* strain			*nusG* strain		
hha	*ydgT*	$-t_{R1}$ (A)	$+t_{R1}$ (B)	% B/A	$-t_{R1}$ (A)	$+t_{R1}$ (B)	% B/A	$-t_{R1}$ (A)	$+t_{R1}$ (B)	% B/A
+	+	7,425 ± 482	493 ± 40	7 ± 0	5,920 ± 700	1,207 ± 230	20 ± 3	5,775 ± 624	1,723 ± 319	30 ± 3
Δ	+	5,683 ± 1,111	497 ± 74	9 ± 1	6,855 ± 160	3,254 ± 399	47 ± 6	6,410 ± 470	1,754 ± 87	27 ± 1
+	Δ	7,564 ± 663	521 ± 62	7 ± 0	6,350 ± 493	3,033 ± 548	48 ± 9	6,627 ± 418	1,553 ± 437	23 ± 6
Δ	Δ	6,110 ± 434	482 ± 39	8 ± 1	ND	ND	ND	6,077 ± 93	2,792 ± 426	46 ± 7

[a] The specific activities of β-galactosidase were determined (after growth in LB medium) for various pairs of strains without ($-t_{R1}$ [A]) or with ($+t_{R1}$ [A]) the phage t_{R1} terminator upstream of the *lacZ* reporter gene. The B/A ratios (%) given in the table are a measure of the transcriptional readthrough or polarity relief at the t_{R1} terminator. The strain pairs ($-t_{R1}/+t_{R1}$) used were as follows (in order, wild type, *rho*, and *nusG*): *hha*$^+$ *ydgT*$^+$, RS445/GJ5147, GJ10570/GJ5146, and GJ10571/GJ5153; Δ*hha ydgT*$^+$, GJ10765/GJ10764, GJ10781/GJ10785, and GJ10767/GJ10766; *hha*$^+$ Δ*ydgT*, GJ10787/GJ10786, GJ10783/GJ10788, and GJ10784/GJ10782; and Δ*hha* Δ*ydgT* (wild-type and *nusG* pairs only), GJ10790/GJ10789 and GJ10791/GJ10792. ND, not determined because of severe growth inhibition associated with *rho* Δ*hha* Δ*ydgT*. See the text for details.

estingly, the ability of H-NSΔ64 to suppress both polarity relief and lethality with pACYC184 was abolished in these derivatives (but not in the *hns* or *stpA* single mutants) (Fig. 4). The plasmid derivative of pACYC184 carrying YdgT (pHYD2546) also conferred lethality in these strains (data not shown), suggesting that neither the H-NS variants nor YdgT can suppress the *rho* and *nusG* phenotypes in strains that are simultaneously deficient for wild-type H-NS and StpA.

Concomitantly, the polarity relief phenotypes associated with *rho* or *nusG* were accentuated by chromosomal deletions of *hha* and *ydgT*, as described below. In the *nusG* strain, polarity relief (at the phage t_{R1} terminator) was unaffected by either of the single perturbations Δ*hha* or Δ*ydgT*, whereas the simultaneous deletion of both conferred enhanced polarity relief (from 30 to 46%) (Table 4); this was also correlated with the loss of suppression by H-NSΔ64 (Fig. 4) or L26P (data not shown) of both polarity relief (at the *trpE* [Fr] locus) and pACYC184 lethality in the *nusG* Δ*hha* Δ*ydgT* strain, presumably because of the increased basal level of termination deficiency in the mutant.

Likewise in the *rho* strain, the introduction of either a Δ*hha* or a Δ*ydgT* single mutation was associated with increased polarity relief at the t_{R1} terminator, from 20% to ca. 48%; furthermore, the *rho* Δ*hha* Δ*ydgT* triple mutant was severely inhibited for growth (Fig. 5). On the other hand, the *rho hns* Δ*stpA* combination was not less healthy than *hns* Δ*stpA* itself (Fig. 5).

H-NS and YdgT perturbations do not increase endogenous levels of Rho and NusG. The results above led us to consider the possibility that the H-NS variants and YdgT overexpression act indirectly, by increasing the expression of Rho or NusG, to restore the efficiency of transcription termination in the *rho* and *nusG* mutants. However, in Western blot experiments with anti-Rho and anti-NusG antibodies, we detected no increase in cytoplasmic levels of Rho or NusG in strains (either *hns*$^+$ or null *hns* on the chromosome) exhibiting suppression of polarity relief on account of expression of H-NSΔ64 or increased YdgT (Fig. 6). Indeed, the opposite effect was observed, whereby the increased levels of Rho that were detected in the *rho* and *nusG* mutants were partially reversed upon H-NSΔ64 or YdgT expression (Fig. 6A, compare lanes 5 and 8 to lanes 2 and 3); since it is known that Rho is autoregulated (31), these results provide yet another line of evidence that H-NSΔ64 and YdgT increase the efficiency of Rho-dependent termination in the mutants.

H-NS and YdgT perturbations do not affect the transcription elongation rate *in vivo*. According to the kinetic coupling model (29), inefficient Rho-dependent termination associated with a *rho* mutation can be rendered more efficient by slowing the rate of transcription elongation. We therefore considered the possibility that the H-NS variants and overexpressed YdgT act to reduce transcription elongation rates *in vivo*, and thus serve to restore the transcription termination efficiency in *rho* and *nusG* strains.

We measured the *in vivo* rates of transcription elongation at the wild-type *lacZ* locus of different strains after IPTG addition, as described previously (10, 29). The results are depicted in Fig. 7, wherein the time point of inflection in each induction curve is an inverse measure of the transcription elongation rate. The data indicate that in comparison with the wild-type strains, the *rho* and *nusG* mutants are unaltered for the rate of transcription elongation (Fig. 7A) and, furthermore, that neither H-NSΔ64 (Fig. 7A) nor YdgT overexpression (Fig. 7B) has any effect in this regard. YdgT overexpression was as-

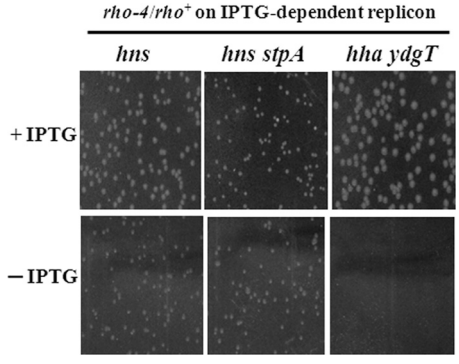

FIG. 5. Synthetic sickness of *rho-4 hha ydgT* mutant. All strains bear the chromosomal *rho-4* mutation and plasmid pHYD1622 (IPTG-dependent replicon with *rho*$^+$), so that the plasmid is retained only in growth medium supplemented with IPTG. The pHYD1622-bearing derivatives of strains GJ10606 (*hns-1001*, marked *hns* in the figure), GJ10663 (*hns stpA*), and GJ10752 (*hha ydgT*) were plated at a suitable dilution on a pair of LB plates without or with IPTG supplementation as marked and then incubated for 16 h (*hns* and *hha ydgT*) or 30 h (*hns stpA*).

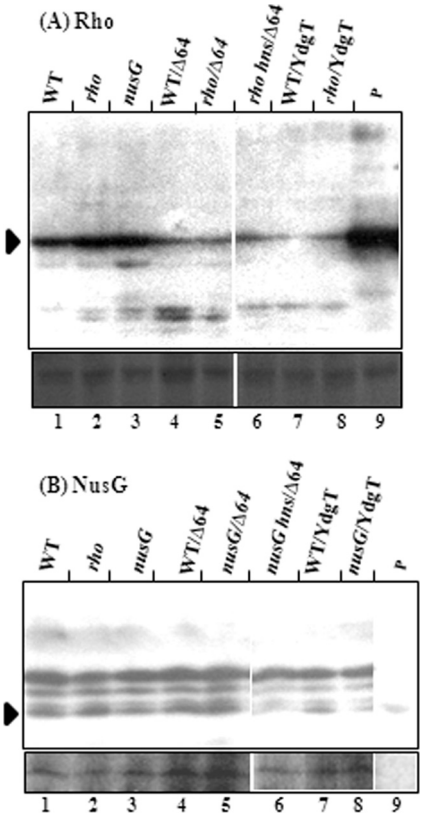

FIG. 6. Immunoblot analysis for intracellular Rho (A) and NusG (B) levels. Strains used were: GJ6504 (wild-type, WT), GJ6509 (*rho*), GJ6511 (*nusG*), GJ10606 (*rho hns*), GJ10607 (*nusG hns*), and their derivatives transformed with pHYD2509 (H-NSΔ64) or pHYD2528 (YdgT). Derivatives with pHYD2528 were grown in IPTG-supplemented medium. All lanes in panel A are from a single gel, as are those in panel B. For each blot, the upper and lower panels show, respectively, the region of specific immunoreactivity with the cognate antibody and a representative slice of the Ponceau-S-stained blot as a loading and transfer control. Lanes marked P in gels A and B represent, respectively, overexpressed Rho and purified NusG proteins (provided by Ranjan Sen), and arrowheads identify the specific immunoreactive band for each antibody.

sociated with a reduced slope of the induction curve in the wild-type strain (Fig. 7B), which was consistent with the data presented in Table 2 suggesting a nonspecific decrease in expression of a *lac* fusion under similar conditions.

DISCUSSION

In this study, we identified several perturbations involving the H-NS family of proteins that affect Rho-dependent transcription termination in *E. coli*. Thus, expression of any one of several dominant-negative variants of H-NS, including Δ64, L26P, and E53G/T55P, restores the efficiency of transcription termination (that is, suppresses polarity relief) in *rho* and *nusG* strains, as does overexpression of YdgT. As reported in an accompanying study (51), a *nusA* mutation associated with defective Rho-dependent termination is also suppressed by H-NSΔ64 and YdgT. These effects are manifest in strains that express wild-type H-NS, StpA or both proteins but not in strains that are simultaneously deficient for H-NS and StpA. The polarity defects associated with the *rho* and *nusG* mutations are rendered more severe in Δ*hha* and Δ*ydgT* derivatives.

The ability of H-NS to influence nucleoid structure and gene expression at the level of transcription initiation has been variously attributed to its different yet inter-related mechanistic properties, including those of high-affinity and low-affinity DNA binding, assembly into a polymeric scaffold, and induction of alterations in DNA architecture such as bending, bridging, stiffening, coating, looping, and supercoiling (16, 20, 23, 32, 39, 61). H-NS has also been implicated in direct RNA binding and translational regulation (41).

Earlier work on dominant-negative H-NS variants has permitted their classification into two categories (5, 58), namely, those that are defective for DNA binding (e.g., Δ64, Δ92, Y97C, P116S, and I119T) and others that are proficient for DNA binding but defective for higher-order oligomerization on DNA (e.g., L26P and E53G/T55P). Both categories of mutations are capable of subunit poisoning of wild-type H-NS to elicit the derepression of H-NS-silenced genes such as *proU*. On the other hand, in the present study, suppression of polarity relief in *rho* and *nusG* mutants was observed with only the second category of dominant-negative mutants and with a limited subset of the first (Δ64). Furthermore, complete deficiency of H-NS, or even that of H-NS and StpA combined, did not confer suppression of polarity relief. These results indicate that the effect of *hns* mutations on modulation of Rho-dependent termination is not completely correlated with that on transcription initiation or gene silencing. A search for genetic suppressors of the effects of H-NS on Rho-dependent termination, as reported in an accompanying study (51), also did not identify any H-NS-repressed gene as being responsible for such modulation. An alternative model is accordingly proposed below.

Modulation of Rho-dependent termination by H-NS: a model. Recent studies have established that H-NS is assembled as a polymeric superhelical scaffold (around which DNA is wrapped) through two oligomerization motifs that are referred to as site 1 and site 2 interfaces, respectively (3, 5, 8, 22, 54, 57, 58). The former involves the N-terminal domain of H-NS (residue 2 to approximately residue 47) and the latter the intermediate or linker domain (residues 58 to 84), and polymerization is achieved by the alternation of site 1-site 1 (head-to-head) and site 2-site 2 (tail-to-tail) interactions between the adjacent protomers in the scaffold (Fig. 8A). Evidence from earlier studies would suggest that the H-NS variant L26P is defective for the former interface (Fig. 8D), while the Δ64 variant is defective for the latter (Fig. 8B). Furthermore, that the other dominant-negative H-NS variants, such as Δ93, Y97C, P116S, and I119T, which are unaffected for transcriptional polarity relief, are proficient for oligomerization through both interfaces (Fig. 8E and F) (3, 5, 8, 22, 54, 57).

We therefore propose that it is the interruption of the linear polymeric scaffold of H-NS and StpA, caused by the recruitment of protomers of Δ64 or L26P into the scaffold, that is specifically required in *cis* for suppression of transcriptional polarity relief in the *rho* and *nusG* mutants, as depicted schematically in Fig. 8B and D, respectively. Modifications of H-NS that interfere with just its DNA-binding properties without affecting scaffold assembly (as shown in Fig. 8E for Δ93 and Fig. 8F for Y97C, P116S, or I119T) would not alter the polarity relief phenotypes of *rho* and *nusG* mutants, and it must be

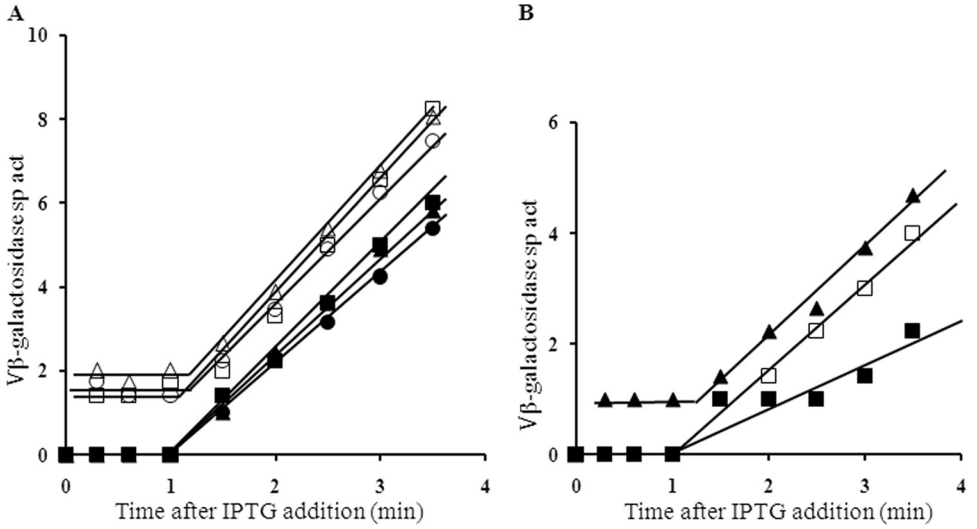

FIG. 7. Transcription elongation rate measurements at *lacZ* locus *in vivo*. β-Galactosidase specific activities were determined at various times after addition of IPTG to each culture grown in 0.4% glycerol–minimal A medium supplemented with Casamino Acids at 0.5% (and additionally 0.2% Ara in the case of strains in panel B), and the inflection point was identified on a curve plotting square root of enzyme specific activity against time, as described previously (10, 29). The strains used were follows: derivatives of MG1655 (wild type, squares), GJ3171 (*rho*, triangles), and GJ10729 (*nusG*, circles) transformed with either the vector pLG339 (open symbols) or its derivative expressing H-NSΔ64 (solid symbols) (A) and MG1655 (wild-type) with either pBAD18 (vector, □) or pHYD2525 (YdgT, ■), and GJ3171 (*rho*) with pHYD2525 (YdgT, ▲) (B). Assays for all strains depicted in a single panel were performed together.

noted here that the recent crystal and solution structure studies (3) indicate that the potential for self-association of H-NS to form the superhelical scaffold exists even in the absence of DNA. We suggest that the E53G/T55P variant of H-NS, which is a suppressor of *rho* and *nusG*, is also affected for one of its two dimerization interfaces, but whether it is site 1 or site 2 which is rendered defective remains to be determined. Our model would also explain an earlier finding that the H-NS variant E74K suppresses the *rho* and *nusG* phenotypes (27), since this variant is expected to be defective for dimerization through the site 2 interface.

Further according to this model, overexpressed YdgT would behave like H-NSΔ64 in serving to interrupt the polymeric scaffold structure by interacting with the N-terminal domain of H-NS, as shown in Fig. 8C. YdgT overexpression was associated also with derepressed *proU* expression, suggesting that proper architecture of the polymer scaffold constituted by the H-NS family of proteins is necessary, but by itself not sufficient, for the gene silencing function (that is, gene regulation could still be defective despite the existence of a proper architecture as, for example, in the case of H-NS variants with substitutions in the DNA-binding domain). A recent report has also implicated H-NS binding in the polymerization or stiffening mode (as opposed to the bridging mode) in silencing of gene expression (61).

The model as proposed establishes a new role for the polymer scaffold of H-NS that is unrelated to the protein's function in silencing of gene expression. The mechanism by which the architecture of the H-NS scaffold affects the process of Rho-dependent termination is not clear. In the kinetic coupling model of Rho action (29), an inefficient Rho can be rendered more effective by slowing the rate of transcription elongation; however, the validity of this model, at least in its simple formulation (29), has recently been questioned since an RNA polymerase mutant with increased elongation rate also exhibited enhanced Rho-dependent termination (21). Moreover, our data reveal no change in RNA polymerase elongation rates *in vivo* in the *rho* and *nusG* strains without or with H-NSΔ64 or overexpressed YdgT, at least on the *lacZ* gene. An alternative possibility is that the nature of the H-NS scaffold influences properties of the transcription elongation complex, such as its stability, pausing behavior, or proneness to backtracking and inactivation (6, 40, 44, 47), and its consequent susceptibility to the process of Rho-dependent termination.

We also found that a deficiency of Hha and YdgT exacerbates the polarity relief phenotypes of *rho* and *nusG* mutants, and indeed that the *rho*(*A243E*) Δ*hha* Δ*ydgT* combination is profoundly growth inhibited. These results suggest that alterations to the H-NS scaffold sculpted even by the native levels of Hha and YdgT are critically important to maintain the residual efficiency of transcription termination needed for robust growth of the *rho* mutant.

Upon testing the single gene knockout collection of *E. coli* (4) for tolerance to different antibiotics, Miller and coworkers found that the Δ*hns* strain is sensitive to the Rho inhibitor bicyclomycin (56). The relevance of this observation to our model remains to be determined, particularly in light of their earlier findings that the Δ*hns* mutant is also sensitive to a variety of other antibiotics, including tetracycline, erythromycin, chloramphenicol, spectinomycin, and rifampin (32).

Finally, how would our model account for the observation that polarity relief conferred by *rho* or *nusG* mutations is unaltered in the *hns*::Kan Δ*stpA* strain, that is, in the complete absence of H-NS and StpA? One possibility is that under these conditions the chromatin architecture is shaped by other proteins such as HU and IHF (16, 20) that do not modulate Rho-dependent termination in the manner that H-NS does. As expected from the model, nevertheless, expression of

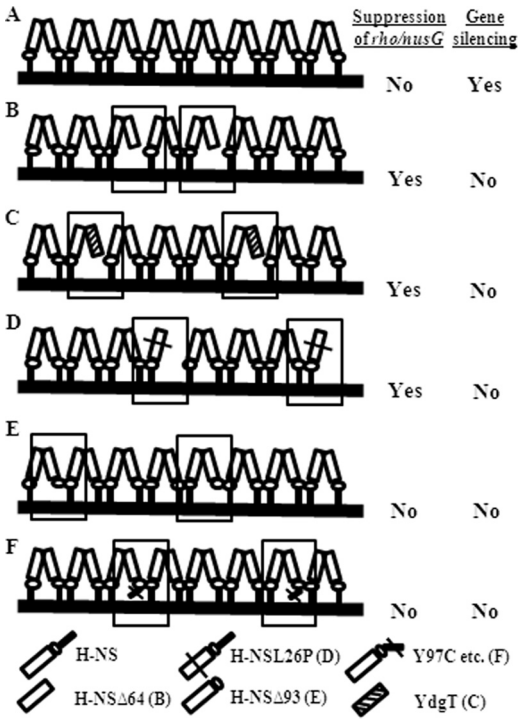

FIG. 8. Diagram representation of the interrupted polymeric scaffold model to explain modulation of Rho-dependent termination by some but not all H-NS variants and by YdgT. DNA is denoted by the horizontal line in all panels, and given in the key are the protomer depictions of H-NS and its variants and of YdgT (with the panel in which each of the variants is inserted mentioned in parentheses). For H-NS, the N-terminal domain (residues 1 to 63), linker or intermediate region (residues 64 to 92), and DNA-binding domain (residues 93 to 137) are represented by the rectangles, ovals, and solid bars, respectively. (A) Wild-type H-NS (and StpA) use two intersubunit contact motifs to form the polymer scaffold from which the DNA-binding domains extend to interact with DNA. The insertion into the scaffold of H-NSΔ64 (B) or YdgT (C) on the one hand, or L26P (D) on the other, leads to its interruption in two alternative ways; insertion of H-NSΔ93 (E) or the other H-NS variants such as Y97C, I119T, or P116S (F) does not affect the scaffold continuity but interferes only with DNA binding. Sites of such insertions into the scaffold are boxed in each panel. Also shown are corresponding effects with respect to (i) suppression of *rho* and *nusG* phenotypes and (ii) ability to silence *proU* gene expression.

H-NSΔ64 did not suppress polarity relief in strains with combined deficiency of H-NS and StpA.

H-NS, Rho, and xenogeneic silencing. Our present results, taken together with recent work from other groups, point to an interesting interplay between H-NS and Rho in the silencing of horizontally acquired or foreign genes (such as those in prophages or pathogenicity islands) in Gram-negative bacteria. H-NS participates in such xenogeneic silencing, and several phages and pathogenicity islands encode proteins that can substitute for, modulate, or even antagonize, H-NS function (reviewed in references 37 and 55). In particular, H-NST is a naturally occurring truncation variant of H-NS whose structure is remarkably similar to H-NSΔ64 (66). Adding to the system's complexity, H-NS also represses the CRISPR mechanism of host immunity against invading phages and plasmids (63).

Intriguingly, Rho-dependent transcription termination is also implicated in promotion of xenogeneic silencing (11), and our results suggest that downregulation of H-NS activity, for example, by a protein such as H-NST, may concomitantly lead to an increased efficiency of Rho-dependent termination. This interplay may therefore be a manifestation of the selection pressures that have acted on hosts and their parasites during the course of biological evolution.

ACKNOWLEDGMENTS

We thank Evelyne Krin, Sylvie Rimsky, Barry Wanner, Ivan Matic, and Ranjan Sen for providing various reagents used in the study and members of the Laboratory of Bacterial Genetics for advice and discussions.

S.S. and J.G. are recipients, respectively, of a doctoral Research Fellowship from the Department of Biotechnology and the J. C. Bose Fellowship from the Department of Science and Technology, Government of India. This study was supported by a Centre of Excellence in Microbial Biology research grant from the Department of Biotechnology.

REFERENCES

1. **Adhya, S., and M. Gottesman.** 1978. Control of transcription termination. Annu. Rev. Biochem. **47:**967–996.
2. **Amann, E., B. Ochs, and K. J. Abel.** 1988. Tightly regulated *tac* promoter vectors useful for the expression of unfused and fused proteins in *Escherichia coli*. Gene **69:**301–315.
3. **Arold, S. T., P. G. Leonard, G. N. Parkinson, and J. E. Ladbury.** 2010. H-NS forms a superhelical protein scaffold for DNA condensation. Proc. Natl. Acad. Sci. U. S. A. **107:**15728–15732.
4. **Baba, T., et al.** 2006. Construction of *Escherichia coli* K-12 in-frame, single-gene knockout mutants: the Keio collection. Mol. Syst. Biol. **2:**1–11.
5. **Badaut, C., et al.** 2002. The degree of oligomerization of the H-NS nucleoid structuring protein is related to specific binding to DNA. J. Biol. Chem. **277:**41657–41666.
6. **Banerjee, S., J. Chalissery, I. Bandey, and R. Sen.** 2006. Rho-dependent transcription termination: more questions than answers. J. Microbiol. **44:**11–22.
7. **Berlyn, M. K.** 1998. Linkage map of *Escherichia coli* K-12, edition 10: the traditional map. Microbiol. Mol. Biol. Rev. **62:**814–984.
8. **Bloch, V., et al.** 2003. The H-NS dimerization domain defines a new fold contributing to DNA recognition. Nat. Struct. Biol. **10:**212–218.
9. **Burmann, B. M., et al.** 2010. A NusE:NusG complex links transcription and translation. Science **328:**501–504.
10. **Burova, E., S. C. Hung, V. Sagitov, B. L. Stitt, and M. E. Gottesman.** 1995. *Escherichia coli* NusG protein stimulates transcription elongation rates in vivo and in vitro. J. Bacteriol. **177:**1388–1392.
11. **Cardinale, C. J., et al.** 2008. Termination factor Rho and its cofactors NusA and NusG silence foreign DNA in *Escherichia coli*. Science **320:**935–938.
12. **Chalissery, J., S. Banerjee, I. Bandey, and R. Sen.** 2007. Transcription termination defective mutants of Rho: role of different functions of Rho in releasing RNA from the elongation complex. J. Mol. Biol. **371:**855–872.
13. **Chalissery, J., et al.** 2011. Interaction surface of the transcription terminator Rho required to form a complex with the C-terminal domain of the antiterminator NusG. J. Mol. Biol. **405:**49–64.
14. **Chang, A. C., and S. N. Cohen.** 1978. Construction and characterization of amplifiable multicopy DNA cloning vehicles derived from the P15A cryptic miniplasmid. J. Bacteriol. **134:**1141–1156.
15. **Ciampi, M. S.** 2006. Rho-dependent terminators and transcription termination. Microbiology **152:**2515–2528.
16. **Dame, R. T.** 2005. The role of nucleoid-associated proteins in the organization and compaction of bacterial chromatin. Mol. Microbiol. **56:**858–870.
17. **Datsenko, K. A., and B. L. Wanner.** 2000. One-step inactivation of chromosomal genes in *Escherichia coli* K-12 using PCR products. Proc. Natl. Acad. Sci. U. S. A. **97:**6640–6645.
18. **Dattananda, C. S., K. Rajkumari, and J. Gowrishankar.** 1991. Multiple mechanisms contribute to osmotic inducibility of *proU* operon expression in *Escherichia coli*: demonstration of two osmoresponsive promoters and of a negative regulatory element within the first structural gene. J. Bacteriol. **173:**7481–7490.
19. **Dersch, P., S. Kneip, and E. Bremer.** 1994. The nucleoid-associated DNA-binding protein H-NS is required for the efficient adaptation of *Escherichia coli* K-12 to a cold environment. Mol. Gen. Genet. **245:**255–259.
20. **Dillon, S. C., and C. J. Dorman.** 2010. Bacterial nucleoid-associated proteins, nucleoid structure and gene expression. Nat. Rev. Microbiol. **8:**185–195.
21. **Epshtein, V., D. Dutta, J. Wade, and E. Nudler.** 2010. An allosteric mechanism of Rho-dependent transcription termination. Nature **463:**245–249.
22. **Esposito, D., et al.** 2002. H-NS oligomerization domain structure reveals the

mechanism for high-order self-association of the intact protein. J. Mol. Biol. **324:**841–850.
23. **Fang, F. C., and S. Rimsky.** 2008. New insights into transcriptional regulation by H-NS. Curr. Opin. Microbiol. **11:**113–120.
24. **Garcia-Contreras, R., X. S. Zhang, Y. Kim, and T. K. Wood.** 2008. Protein translation and cell death: the role of rare tRNAs in biofilm formation and in activating dormant phage killer genes. PLoS One **3:**e2394.
25. **Gowrishankar, J., and R. Harinarayanan.** 2004. Why is transcription coupled to translation in bacteria? Mol. Microbiol. **54:**598–603.
26. **Guzman, L. M., D. Belin, M. J. Carson, and J. Beckwith.** 1995. Tight regulation, modulation, and high-level expression by vectors containing the arabinose PBAD promoter. J. Bacteriol. **177:**4121–4130.
27. **Harinarayanan, R., and J. Gowrishankar.** 2003. Host factor titration by chromosomal R-loops as a mechanism for runaway plasmid replication in transcription termination-defective mutants of *Escherichia coli*. J. Mol. Biol. **332:**31–46.
28. **Hommais, F., et al.** 2001. Large-scale monitoring of pleiotropic regulation of gene expression by the prokaryotic nucleoid-associated protein, H-NS. Mol. Microbiol. **40:**20–36.
29. **Jin, D. J., R. R. Burgess, J. P. Richardson, and C. A. Gross.** 1992. Termination efficiency at rho-dependent terminators depends on kinetic coupling between RNA polymerase and *rho*. Proc. Natl. Acad. Sci. U. S. A. **89:**1453–1457.
30. **Kim, M. S., et al.** 2005. Cnu, a novel *oriC*-binding protein of *Escherichia coli*. J. Bacteriol. **187:**6998–7008.
31. **Kung, H., et al.** 1984. Autoregulation of the *rho* gene of *Escherichia coli* K-12. Mol. Gen. Genet. **193:**210–213.
32. **Liu, Y., H. Chen, L. J. Kenney, and J. Yan.** 2010. A divalent switch drives H-NS/DNA-binding conformations between stiffening and bridging modes. Genes Dev. **24:**339–344.
33. **Madrid, C., C. Balsalobre, J. Garcia, and A. Juarez.** 2007. The novel Hha/YmoA family of nucleoid-associated proteins: use of structural mimicry to modulate the activity of the H-NS family of proteins. Mol. Microbiol. **63:**7–14.
34. **Martin, W., and E. V. Koonin.** 2006. A positive definition of prokaryotes. Nature **442:**868.
35. **Miller, J. H.** 1992. A short course in bacterial genetics: a laboratory manual and handbook for *Escherichia coli* and related bacteria. Cold Spring Harbor Laboratory, Cold Spring Harbor, NY.
36. **Mooney, R. A., K. Schweimer, P. Rosch, M. Gottesman, and R. Landick.** 2009. Two structurally independent domains of *Escherichia coli* NusG create regulatory plasticity via distinct interactions with RNA polymerase and regulators. J. Mol. Biol. **391:**341–358.
37. **Navarre, W. W., M. McClelland, S. J. Libby, and F. C. Fang.** 2007. Silencing of xenogeneic DNA by H-NS: facilitation of lateral gene transfer in bacteria by a defense system that recognizes foreign DNA. Genes Dev. **21:**1456–1471.
38. **Nieto, J. M., et al.** 2002. Evidence for direct protein-protein interaction between members of the enterobacterial Hha/YmoA and H-NS families of proteins. J. Bacteriol. **184:**629–635.
39. **Noom, M. C., W. W. Navarre, T. Oshima, G. J. Wuite, and R. T. Dame.** 2007. H-NS promotes looped domain formation in the bacterial chromosome. Curr. Biol. **17:**R913–R914.
40. **Nudler, E., and M. E. Gottesman.** 2002. Transcription termination and anti-termination in *Escherichia coli*. Genes Cells **7:**755–768.
41. **Park, H. S., Y. Ostberg, J. Johansson, E. G. Wagner, and B. E. Uhlin.** 2010. Novel role for a bacterial nucleoid protein in translation of mRNAs with suboptimal ribosome-binding sites. Genes Dev. **24:**1345–1350.
42. **Paytubi, S., et al.** 2004. YdgT, the Hha paralogue in *Escherichia coli*, forms heteromeric complexes with H-NS and StpA. Mol. Microbiol. **54:**251–263.
43. **Peters, J. M., et al.** 2009. Rho directs widespread termination of intragenic and stable RNA transcription. Proc. Natl. Acad. Sci. U. S. A. **106:**15406–15411.
44. **Peters, J. M., A. D. Vangeloff, and R. Landick.** 2011. Bacterial transcription terminators: the RNA 3′-end chronicles. J. Mol. Biol. doi:10.1016/j.jmb.2011.03.036.
45. **Proshkin, S., A. R. Rahmouni, A. Mironov, and E. Nudler.** 2010. Cooperation between translating ribosomes and RNA polymerase in transcription elongation. Science **328:**504–508.
46. **Rajkumari, K., S. Kusano, A. Ishihama, T. Mizuno, and J. Gowrishankar.** 1996. Effects of H-NS and potassium glutamate on σ^S- and σ^{70}-directed transcription in vitro from osmotically regulated P1 and P2 promoters of *proU* in *Escherichia coli*. J. Bacteriol. **178:**4176–4181.
47. **Richardson, J. P.** 2002. Rho-dependent termination and ATPases in transcript termination. Biochim. Biophys. Acta **1577:**251–260.
48. **Rudd, K. E.** 1998. Linkage map of *Escherichia coli* K-12, edition 10: the physical map. Microbiol. Mol. Biol. Rev. **62:**985–1019.
49. **Sambrook, J., and D. W. Russell.** 2001. Molecular cloning: a laboratory manual, 3rd ed. Cold Spring Harbor Laboratory, Cold Spring Harbor, NY.
50. **Santangelo, T. J., et al.** 2008. Polarity in archaeal operon transcription in *Thermococcus kodakaraensis*. J. Bacteriol. **190:**2244–2248.
51. **Saxena, S., and J. Gowrishankar.** 2011. Compromised factor-dependent transcription termination in a *nusA* mutant of *Escherichia coli* and spectrum of termination efficiencies generated by perturbations of Rho, NusG, NusA, and H-NS family proteins. J. Bacteriol. **193:**3842–3850.
52. **Sen, R., J. Challissery, and G. Muteeb.** 18 January 2008, posting date. Module 4.5.3.1, Nus factors of *Escherichia coli*. *In* R. Curtiss III et al. (ed.), EcoSal—*Escherichia coli* and *Salmonella*: cellular and molecular biology. ASM Press, Washington, DC. http://www.ecosal.org/.
53. **Sonden, B., and B. E. Uhlin.** 1996. Coordinated and differential expression of histone-like proteins in *Escherichia coli*: regulation and function of the H-NS analog StpA. EMBO J. **15:**4970–4980.
54. **Stella, S., R. Spurio, M. Falconi, C. L. Pon, and C. O. Gualerzi.** 2005. Nature and mechanism of the in vivo oligomerization of nucleoid protein H-NS. EMBO J. **24:**2896–2905.
55. **Stoebel, D. M., A. Free, and C. J. Dorman.** 2008. Anti-silencing: overcoming H-NS-mediated repression of transcription in Gram-negative enteric bacteria. Microbiology **154:**2533–2545.
56. **Tran, L., J. A. van Baarsel, R. S. Washburn, M. E. Gottesman, and J. H. Miller.** 2011. Single-gene deletion mutants of *Escherichia coli* with altered sensitivity to bicyclomycin, an inhibitor of transcription termination factor rho. J. Bacteriol. **193:**2229–2235.
57. **Ueguchi, C., C. Seto, T. Suzuki, and T. Mizuno.** 1997. Clarification of the dimerization domain and its functional significance for the *Escherichia coli* nucleoid protein H-NS. J. Mol. Biol. **274:**145–151.
58. **Ueguchi, C., T. Suzuki, T. Yoshida, K. Tanaka, and T. Mizuno.** 1996. Systematic mutational analysis revealing the functional domain organization of *Escherichia coli* nucleoid protein H-NS. J. Mol. Biol. **263:**149–162.
59. **Ussery, D. W., et al.** 1994. The chromatin-associated protein H-NS. Biochimie **76:**968–980.
60. **Uyar, E., et al.** 2009. Differential binding profiles of StpA in wild-type and *hns* mutant cells: a comparative analysis of cooperative partners by chromatin immunoprecipitation-microarray analysis. J. Bacteriol. **191:**2388–2391.
61. **Walthers, D., et al.** 2011. *Salmonella enterica* response regulator SsrB relieves H-NS silencing by displacing H-NS bound in polymerization mode and directly activates transcription. J. Biol. Chem. **286:**1895–1902.
62. **Wang, R. F., and S. R. Kushner.** 1991. Construction of versatile low-copy-number vectors for cloning, sequencing and gene expression in *Escherichia coli*. Gene **100:**195–199.
63. **Westra, E. R., et al.** 2010. H-NS-mediated repression of CRISPR-based immunity in *Escherichia coli* K-12 can be relieved by the transcription activator LeuO. Mol. Microbiol. **77:**1380–1393.
64. **Whitman, W. B.** 2009. The modern concept of the procaryote. J. Bacteriol. **191:**2000–2005.
65. **Williams, R. M., S. Rimsky, and H. Buc.** 1996. Probing the structure, function, and interactions of the *Escherichia coli* H-NS and StpA proteins by using dominant-negative derivatives. J. Bacteriol. **178:**4335–4343.
66. **Williamson, H. S., and A. Free.** 2005. A truncated H-NS-like protein from enteropathogenic *Escherichia coli* acts as an H-NS antagonist. Mol. Microbiol. **55:**808–827.
67. **Zhang, A., S. Rimsky, M. E. Reaban, H. Buc, and M. Belfort.** 1996. *Escherichia coli* protein analogs StpA and H-NS: regulatory loops, similar and disparate effects on nucleic acid dynamics. EMBO J. **15:**1340–1349.